Molecular Approach to Electrochemically Switchable Monolayer MoS2 Transistors

Yuda Zhao, Simone Bertolazzi, Maria Serena Maglione, Concepció Rovira, Marta Mas-Torrent, Paolo Samorì

▶ **To cite this version:**

Yuda Zhao, Simone Bertolazzi, Maria Serena Maglione, Concepció Rovira, Marta Mas-Torrent, et al.. Molecular Approach to Electrochemically Switchable Monolayer MoS2 Transistors. Advanced Materials, Wiley-VCH Verlag, 2020, pp.2000740. 10.1002/adma.202000740 . hal-02562795

HAL Id: hal-02562795

https://hal.archives-ouvertes.fr/hal-02562795

Submitted on 4 May 2020

HAL is a multi-disciplinary open access archive for the deposit and dissemination of scientific research documents, whether they are published or not. The documents may come from teaching and research institutions in France or abroad, or from public or private research centers.

L'archive ouverte pluridisciplinaire **HAL**, est destinée au dépôt et à la diffusion de documents scientifiques de niveau recherche, publiés ou non, émanant des établissements d'enseignement et de recherche français ou étrangers, des laboratoires publics ou privés.

Molecular Approach to Electrochemically Switchable Monolayer MoS_2 Transistors

*Yuda Zhao, Simone Bertolazzi, Maria Serena Maglione, Concepció Rovira, Marta Mas-Torrent, Paolo Samorì**

Dr. Yuda Zhao, Dr. Simone Bertolazzi, Prof. Paolo Samorì
University of Strasbourg, CNRS, ISIS UMR 7006, 8 allée Gaspard Monge, F-67000 Strasbourg, France
Email: samori@unistra.fr

Dr. Maria Serena Maglione, Prof. Concepció Rovira, Prof. Marta Mas-Torrent
Institut de Ciència de Materials de Barcelona (ICMAB-CSIC) and Networking Research Center on Bioengineering Biomaterials and Nanomedicine (CIBER-BBN), Campus de la UAB, 08193 Bellaterra, Spain

Keywords: 2D semiconductors, molecular switches, electrochemically switchable transistors, functional devices, subthreshold swing

Abstract

As the Moore's law is running to its physical limit, tomorrow's electronic system can be leveraged to a higher value by integrating "More than Moore" technologies into CMOS digital circuits. The hybrid heterostructure composed of two-dimensional (2D) semiconductors and molecular materials represents a powerful strategy to confer new properties to the former components, realize stimuli-responsive functional devices and enable diversification in "More than Moore" technologies. Here, we fabricated an ionic liquid-gated 2D MoS_2 field-effect transistor (FET) with molecular functionalization. The suitably designed ferrocene substituted alkanethiol molecules do not only improve the FET performance, but they also show reversible electrochemical switching on MoS_2 surface. Field-effect mobility of monolayer MoS_2 reaches values as high as ~116 $cm^2V^{-1}s^{-1}$ with I_{on}/I_{off} ratio exceeding 10^5. Molecules in their neutral or charged state impose distinct doping effect, efficiently tuning the electron density in monolayer MoS_2. It is noteworthy that the joint doping effect from ionic liquid and switchable molecules results in the steep subthreshold swing of MoS_2 FET in the backward sweep. These results demonstrate that our device architecture represents an unprecedented and powerful strategy to

fabricate switchable 2D FET with chemically programmed electrochemical signal as remote control, paving the road towards novel functional devices.

Introduction

Two-dimensional (2D) semiconductors combine several unique properties including atomic thickness, sizable bandgap, absence of dangling bonds, and high carrier mobility making them ideal building blocks for the next generation of ultrathin-body field effect transistors (FETs).[1-3] In the post-silicon microelectronics, 2D semiconductors show the advantages to break through the scaling limits, continuously minimize the device size, and simultaneously preserve the device performance.[4-6] As a basic electronic device, 2D FET represents not only the building block for integrated circuits, but it can also operate as the key element in functional devices, such as chemical sensors and emerging memory devices.[7-10] Therefore, 2D semiconductor FETs have become the keystone for novel functional devices.

Albeit unique and outstanding, the properties of 2D semiconductors can be hardly tuned in a controllable manner via the conventional semiconductor technologies. However, the combination of 2D semiconductors with molecular materials represents a powerful strategy to confer new properties to the former components. A nice proof of this concept was reported by combining photochromic molecules and 2D materials to form light-switchable hybrid van der Waals (vdW) heterostructures,[11-13] which have been successfully exploited as channel materials in FETs to construct stimuli-responsive functional devices, including optically controlled FET, optical memory, and optically tunable *p-n* diode.[14-16] These achievements greatly promote the development of 2D hybrid systems in the field of optoelectronics. Alongside light, the electrochemical stimulus represents another powerful input to reversibly switch the state of suitably designed molecules.[17-19] In a micro-electrochemical cell, 2D semiconductors can work as the electrode to monitor electrochemical reactions of the switchable molecules occurring at the interface, which is crucial for both fundamental studies

and chemical sensing applications. Among various properties that can be changed as a result of electrochemical switching, the possibility to influence the charge transport on the nearby 2D layers by proper design, open intriguing perspectives towards the realization of remote-controlled FETs responding to electrochemical signals.

Here, we demonstrate the reversible switching of ferrocene-substituted hexanethiol molecules adsorbed on the MoS_2 surface, which can be directly monitored in ionic liquid (IL)-gated MoS_2 FETs. In particular, molecules with the ferrocene group in the neutral or oxidized state can induce different doping effects, which effectively tune the charge transport in the underlying MoS_2 layer. This doping effect results from the electrostatic gating from the charged/neutral molecules. Thanks to the synergetic effect from both IL and the electroactive molecules, we surprisingly observe the ultra-steep subthreshold swing in the backward sweep. All these results indicate that our novel device platform has huge technological potential for the development of electrochemically switchable 2D devices and provides an enlightening guidance on electrochemical sensing devices.

Results

As prototypical electrochemical switching molecule for the functionalization of transition metal dichalcogenides (TMDs), we have focused our attention to a commercial ferrocene-terminated alkanethiol molecule, i.e. 6-(ferrocenyl)hexanethiol (Fc-SH). Its special design comprises an electrochemically switchable ferrocene unit grafted at the end of an alkyl thiol, the latter being capable of chemisorption on TMDs with sulfur vacancies to form functional heterostructure. The scheme of the device architectures is portrayed in **Figure 1**a. A back-gate monolayer MoS_2 FET was fabricated on the SiO_2/Si substrate with Au metal electrodes. A thin layer of insulating lithium fluoride (LiF) was deposited on Au metal electrodes to prevent its interaction with the molecules and IL. Then Fc-SH molecules were spin-coated on the 2D surface, yielding a mixture of chemisorbed and physisorbed molecular layer. The insulating LiF layer prevents the

chemisorption of molecules on Au electrodes, thereby minimizing the work function change of Au electrodes. The effect induced by molecules on the transfer characteristics of MoS_2 FET is displayed in Figure 1b. The functionalization increases the on-current level and improves the field-effect mobility (from 15 to 36 $cm^2V^{-1}s^{-1}$). The output curves (Figure 1c) preserve the linear relationship under low drain biases (V_d < 0.1 V), demonstrating a relatively low contact resistance. On the one hand, the thiol functional groups can heal the sulfur vacancies in transition metal disulfides, thereby suppressing the electron scattering around defective sites;[20, 21] on the other hand, the increased electron density in MoS_2 via the molecular doping effect can decrease the contact resistance. Ultimately, these two factors together improve the FET performance. In order to verify the healing efficacy of the molecules, the same experiment was performed on ion-irradiated MoS_2 devices with a 3% generated vacancy density. The vacancy generation and characterization method is systematically described in our previous work.[21] After molecular treatment, a remarkable drain current recovery in the transfer characteristics (Figure 1d) was obtained from the ion-irradiated device with I_{on}/I_{off} ratio enhanced from ~4×10^3 to ~2×10^5 and field-effect mobility grown from ~0.01 to ~0.2 $cm^2V^{-1}s^{-1}$. Photoluminescence (PL) and Raman spectroscopy measurements provide independent and unambiguous further evidence for the defect healing (Figure S1). After molecular adsorption, the defect-mediated emission peak at 1.76 eV remarkably decreases in PL spectra and the disorder-activated side bands of E_{2g}^1 mode show a damping trend in Raman spectra.[22, 23] As a control experiment, the adsorption of unsubstituted ferrocene molecules (Fc, formula $Fe(C_5H_5)_2$), i.e. with neither thiol group nor alkyl chain, on the pristine MoS_2 FET did not reveal improvement/recovering of the device's electrical properties but rather show *p*-doping effect (Figure S2). Overall, Fc-SH molecules are capable of chemisorption on MoS_2 to form functional heterostructure with improved device performance.

After the adsorption of Fc-SH molecules on the MoS_2 FET, a small droplet of ionic liquid (IL), i.e. diethylmethyl(2-methoxyethyl)ammonium bis(trifluoromethylsulfonyl)imide (DEME-

TFSI), was applied onto the devices, covering the MoS_2 channel. The top-gate electrode (Pt wire) was immersed in the IL (**Figure 2**a). The voltage applied on the top-gate electrode (V_{ig}) can effectively modulate the carrier density in monolayer MoS_2 by forming the electrical double layers at the interfaces between IL and monolayer MoS_2 and IL and the gate electrode. Figure 2b shows the transfer characteristics of top-gate monolayer MoS_2 FET at the drain-source voltage V_d of 0.01 V and back-gate voltage V_{bg} of 0 V. The device exhibits unipolar n-type transport behavior, with the I_{on}/I_{off} ratio exceeding 10^5. To extract the electron mobility, we first estimate the capacitance of IL by measuring I_d versus V_{ig} at various fixed back-gate voltages V_{bg} in a dual gate transistor configuration (Figure S3). The result shows that the estimated capacitance of IL (C_{ig}) is ~6.4 μF/cm^2 and the extracted field-effect mobility of MoS_2 is ~116 cm^{2}V^{-1}s^{-1}, being ~3 times larger than that from back-gate device. The high carrier mobility can be attributed to the high electron injection in MoS_2 via the gating effect from IL, which induces the Schottky barrier thinning, improves electron tunneling from electrode, and greatly reduces the contact resistance.[24] The drain current drop at high electron density condition ($V_g > 0.5$ V) is mostly attributed to the increased interband scattering in MoS_2.[25] Surprisingly, we observe the subthreshold swing (SS) of top-gate device amounts to 49 mV/decade in the backward sweep of gate voltage (from positive to negative), which is less than the theoretical limit 60 mV/decade at 300 K.[26, 27] Such a phenomenon will be discussed in detail in the latter part of this paper.

The device is essentially a two-electrode micro-electrochemical cell with MoS_2 operating as the working electrode and Pt wire as the counter electrode (Figure 2c). The IL provides the electrolyte environment for electrochemical reactions. As a simple electrochemically switchable molecule, unsubstituted ferrocene is capable of undergoing redox switching in the IL, an unconventional kind of electrolyte, with highly reproducible electrochemical behavior.[28-30] In our system, the electrochemically switching behavior of Fc-SH molecules is studied once adsorbed onto the monolayer MoS_2 electrode via the cyclic voltammogram (CV) by

sweeping the potential of Pt counter electrode relative to the working electrode (scan rate 16.7 mV/s) at V_{bg} = 0 V. In the meanwhile, a small constant voltage bias (0.01 V) is applied between two Au electrodes on MoS_2 to measure the electrical transport properties of MoS_2 layer. In Figure 2d, the quasi-reversible CV characteristics with the reduction and oxidation peaks are observed at 0.55 V and 0.825 V, respectively. These two redox peaks can be attributed to the chemically reversible one-electron oxidation/reduction of ferrocene electroactive core, as shown in Equation 1:[31]

$$\text{Fc-SH} \rightleftharpoons \text{Fc}^{+}\text{-SH} + \text{e}^{-} \quad (1)$$

The $Fc^{0/+}$ electron transfer reaction occurs across the MoS_2/IL interface via a heterogeneous process. Therefore, the electrochemical state of ferrocene functional group can be programmed by tuning the working electrode potential (i.e. the voltage applied on the Pt electrode). As a blank test, the electrical characterizations were performed on the IL-gated pristine MoS_2 FET without molecular adsorption. The transistor shows typical transfer characteristics, but no redox peaks can be observed from the CV curve (Figure S4). Another control experiment was performed on the IL-gated MoS_2 FET with the adsorption of unsubstituted Fc molecules. Redox peaks can be observed from the CV curve (Figure S5), demonstrating that ferrocene functional group in Fc-SH is responsible for the switching behavior.

Since Fc and Fc^+ are uncharged and monocationic species, respectively, they can be expected to yield different doping effect on the adjacent MoS_2 layers. However, two synergetic factors contribute to current modulation in MoS_2 FET from top-gate operation, being IL gating and molecular doping. The direct observation of the molecular doping effect is rather complicated because the electrostatic gating from IL with large capacitance makes the majority contribution to carrier modulation in MoS_2. In order to easily monitor the molecular doping effect, we change the device characterization structure from top-gate to back-gate configuration. In particular, the electrochemical state of Fc-SH molecules is first set by a top-gate voltage applied on the Pt electrode, such as -0.8 V applied on Pt electrode (working electrode potential vs Pt is

+0.8 V in Figure 2d) to convert the uncharged Fc-SH to the oxidized state Fc^+-SH, or +0.2 V applied on Pt electrode (working electrode potential vs Pt is -0.2 V in Figure 2d) to trigger the charged Fc^+-SH back to the uncharged Fc-SH state. After programming the molecules into different electrochemical states (Fc-SH or Fc^+-SH) by the top gate, the electrical transport behavior of monolayer MoS_2 with different molecular doping condition can be detected from the back-gate configuration (**Figure 3**a). Figure 3b shows a representative reversible doping cycle on monolayer MoS_2 FET with Fc-SH adsorption. After switching the molecules from the neutral Fc-SH to the charged Fc^+-SH state, an increase of drain current in the transfer curves from the back-gate configuration can be observed accompanied by a shift of the threshold voltage towards the negative direction ($\Delta V_{th} = -13.75$ V, compared with neutral Fc-SH state). The drain current increases ~25% at $V_{bg} = 90$ V and the current ratio of MoS_2 with Fc^+-SH and Fc-SH adsorption is over 2 at $V_{bg} = -50$ V. Therefore, Fc^+-SH molecules accumulate the electron carriers and induce *n*-type doping on MoS_2. The increased electron concentration induced by Fc^+-SH molecules is ~1.10×10^{12} cm^{-2}. The charged molecules can be toggled back to the neutral Fc-SH state by applying +0.2 V on Pt electrode. After doing this, the drain current and threshold voltage from the back-gate FET get restored almost to the original values. These results demonstrate that the doping effect from the electrochemically switchable Fc-SH molecules on monolayer MoS_2 is controllable and reversible. As a blank test, the electrical characterizations were performed on the MoS_2 FET without molecular adsorption. The test procedure is the same, i.e. that top-gate voltage is first applied, then it is removed, and last the device is measured from the back-gate configuration. The back-gate transfer curves of MoS_2 FET (Figure S6) are nearly coincident during the whole test, excluding the extrinsic factors in modulating the carrier concentration of MoS_2.

Besides the electrical characterization, the photoluminescence (PL) spectra can be used to monitor the admolecules induced doping of monolayer MoS_2. Figure 3c compares the PL spectra of monolayer MoS_2 when the adsorbed molecules are either neutral or charged. The A

peak is fitted with the contribution from both neutral excitons and negatively charged excitons (trions). The spectral weight of trion is directly related to the amount of electron doping in monolayer MoS_2.[32, 33] The results show that the trion weight of A peak in MoS_2 with neutral Fc-SH adsorption is ~0.43 and it increases to ~0.56 with charged Fc^+-SH adsorption. The increased trion spectra weight in the integrated A peak clearly suggests that charged Fc^+-SH molecules induce *n*-type doping, which is consistent with the electrical results.

In our device system, the molecular state can be first set by applying a constant voltage on the Pt electrode. Once the top-gate voltage on Pt electrode is removed, the adsorbed molecules maintain their electrochemical states and the MoS_2 layer is doped without the influence from IL. The positively charged molecules can induce the accumulation of electrons in the adjacent MoS_2 layer (Figure 3d), hence *n*-type doping effect. Therefore, in our device system, the top gate is used to electrochemically program the state of the Fc-SH molecules, while the reversible and controllable doping of MoS_2 by the switchable Fc-SH molecules can be demonstrated from the back-gate electrical characterization. A detailed schematic diagram in Figure S7 depicts the dual functions of top-gate voltage applied on the Pt electrode in our IL-gated FET.

The steep subthreshold swing (SS) has received increased attention because of the urgent need for low power dissipation and high energy efficiency in modern electronics. One of the main obstacles lays on the intrinsic physical limit of SS in conventional FETs, which cannot be reduced below 60 mV/decade at room temperature. Here, we show the expression of SS in Equation 2:[26, 27]

$$SS = \ln 10 \frac{kT}{q}\left(1 + \frac{C_d}{C_{ox}}\right) \tag{2}$$

$$\rightarrow \ln 10 \frac{kT}{q} = 60\ mV/decade, at\ T = 300\ K$$

where kT/q is the thermal voltage and C_d and C_{ox} are the depletion and the dielectric capacitances, respectively. Therefore, the sub-60 mV/decade SS need to be obtained by using new physical principles rather than thermionic injection.

In our IL-gated FET with Fc-SH adsorption, the forward-sweep SS shows a value exceeding 60 mV/decade, whereas the backward-sweep SS is reduced to a minimum of 49 mV/decade (**Figure 4**a). The sub-60 mV/decade SS is kept for current change by nearly two orders of magnitude in the backward sweep (Figure 4b). The IL-gated FET with unsubstituted Fc adsorption (Figure S8) also displays a minimum of 50 mV/decade SS in the backward sweep. As a blank test, the IL-gated FET without molecules shows the SS with the value of ~71 mV/decade in both directions (Figure S9). All these results demonstrate that the large IL capacitance contributes to a relatively small SS (~71 mV/decade without molecular adsorption) and the additional molecular interaction is critical to the reduced SS effect, especially due to the electrochemically switchable ferrocene group.

Several novel FET structures have been proposed to generate sub-60 mV/decade SS, such as tunnel FET,[34, 35] impact-ionization FET,[36] suspended-gate FET,[37] and negative-capacitance FET.[38, 39] Besides the widely used ferroelectric materials in stacked dielectric layers,[40, 41] charge trapping in oxide dielectric is recently reported to achieve the negative capacitance and sub-60 mV/decade SS in FET.[42] Different from the random charge trapping/de-trapping process in the oxide,[42] in our device system the adsorbed molecules act as the specially designed charge trapping sites, which can be electrochemically switched between the charged and neutral states via the redox reaction in the IL dielectric. The positively charged molecules in the IL can modify the surface potential of 2D semiconductors via the coupled capacitance effect and induce the accumulation of electrons. In Figure 4a, in the subthreshold region marked by yellow background, the applied IL-gate voltage in the range from -0.24 V to -0.12 V can reduce the charged Fc^+-SH to the neutral Fc-SH molecules and modulate the adsorption condition of charged species at the MoS_2 working electrode. Therefore, in the backward sweep, the reduced SS with sub-60 mV/decade is caused by simultaneous reduction of positively charged Fc^+-SH molecules (hence, depletion of 2D semiconductor due to molecules) and the semiconductor transition from accumulation to depletion (due to IL gating).

In order to minimize the influence from IL, we can slow down the scan rate of the applied IL-gate voltage to effectively control the diffusion of ions in IL. The slow scan rate results in the reduced hysteresis of the transfer curves from 79 mV (fast, 16.7 mV/s) to 16 mV (slow, 1.66 mV/s) at I_d = 10 nA (Figure 4c). It is worth noting that the scan rate shows weak influence on the minimum SS value, which is kept less than 60 mV/decade in the backward sweep within our measured scan rate (Figure 4d). When the scan voltage range decreases from ±1 V to ±0.5 V, the transfer curve in Figure 4e shows smaller hysteresis, and the CV curve in the inset of Figure 4e exhibits the reduced redox peak currents, demonstrating the decreased number of molecules that undergo reversible electrochemical reactions. This will directly influence the reduced SS effect, showing an increase of the minimum SS in the backward sweep from 55 mV/dec to 61 mV/dec in Figure 4f. The same measurements on the IL-gated FET without molecules in Figure S10 show that the SS value (> 80 mV/dec) are less dependent on the scan voltage range. Overall, the comparison of SS value between devices with and without molecular adsorption under different scan rate and different scan range of IL-gate voltage demonstrates the crucial role of electrochemically switchable molecules in the reduced SS effect.

Compared with the FET in absence of adsorbed molecules, the IL-gate current in FET in presence of adsorbed Fc-SH increases due to the redox reactions of Fc-SH molecules. However, such a leakage current is around 4 orders of magnitude smaller than the on-state drain current, demonstrating its negligible contribution when the transistor is turned on. When operating in the subthreshold region of MoS_2 FET two effects take place. On the one hand, the switching of redox molecules results in the steep subthreshold swing. On the other hand, the IL-gate current contributes to the drain current (especially near the off-state), limiting the current range with sub-60 mV/decade SS in the backward sweep. The further study of the negative capacitance in our device architecture and the detailed physical model to understand the reduced SS effect will be a subject of future research. Although the SS hysteresis imposes an obstacle for the practical application in low-power devices, our device system provides a novel platform to investigate

ultra-steep SS effect and benefit from the controllable charge trapping/release process it can function as a memory device. The device also holds potential for its application in electrochemical sensing and biosensing, with a higher sensitivity expected to be achieved during the device operation in (deep) subthreshold regime.[43]

Although both Fc-SH and unsubstituted Fc molecules show the electrochemically switchable behavior in IL dielectric and tunable doping effect on 2D semiconductors (Figure S11), the two device systems display different stability and fatigue resistance. Figure S12 displays the IL-gated transfer curves and gate current curves of MoS_2 FET with Fc-SH or unsubstituted Fc adsorption at different sweep cycles. When Fc-SH adlayers are used, the molecular switchable behavior has been observed from the 1st sweep cycle and it remains relatively stable until the 20^{th} sweep cycle. Atomic force microscopy imaging further provides unambiguous evidence of the good stability of MoS_2 flake which does not exhibit noticeable damage after the electrochemically switching process, as illustrated in Figure S13. In contrast, when the unsubstituted Fc adlayers are employed, the charge transfer between molecules and MoS_2 working electrode is unstable and gate current curves exhibit notable variations. Such a difference can be ascribed to the ability of Fc-SH molecules to heal the sulfur vacancies in monolayer MoS_2 leading to improved stability of MoS_2 working electrode in the IL electrochemical system. Alongside, Fc-SH molecules are also prone to physisorb onto the surface of 2D layers due to the alkyl chain, which is beneficial to form a stable adsorption layer. Therefore, the different adsorption types of molecules on MoS_2 can effectively change the switching stability of molecules and the charge transport in the 2D materials, further demonstrating the important role of molecules in the gating effect and reduced SS effect.

Conclusion

In summary, in this work we have realized the in-situ programming of molecular states by fabricating the IL-gated FET device with an electrochemically switchable molecular adlayer

onto the 2D semiconductor channel and further demonstrated for the first time the tunable molecular doping effect on the electrical transport of 2D semiconductors via electrochemical stimuli. The thiol group in Fc-SH molecules can improve the FET performance by healing the sulfur vacancies of monolayer MoS_2, while the ferrocene group in the molecules is responsible for the tunable doping on 2D semiconductor via reversible switching between neutral and positively charged states. Both the electrical transport measurement and spectroscopic characterization provided unambiguous evidence for the reversible doping of monolayer MoS_2 by tuning the electrochemical states of molecules. Noteworthy, the superimposed molecular doping effect on the conventional IL electrostatic gating effect results in the ultra-steep SS with sub-60 mV/decade. The novel device architecture demonstrates the unique multifunctional nature of monolayer MoS_2 FETs via electrochemical responsivity. Our switchable device with new analog functions adds diversification in electronic systems and promotes the development of "More than Moore" technologies.

Experimental Section

Experimental details are available in the Supporting Information.

Supporting Information

Supporting Information is available from the Wiley Online Library or from the author.

Acknowledgements

Device fabrication was carried out in part at the nanotechnology facility eFab (IPCMS, Strasbourg). We acknowledge funding from European Commission through the ERC project SUPRA2DMAT (GA-833707), the Marie-Curie IEF STELLAR (GA-795615), the Graphene Flagship Core 2 project (GA-785219), the Marie Sklodowska-Curie project ITN project iSwitch (GA-642196), the Agence Nationale de la Recherche through the Labex projects CSC (ANR-10-LABX-0026 CSC) and NIE (ANR-11-LABX-0058 NIE) within the Investissement d'Avenir program (ANR-10-120 IDEX-0002-02), the International Center for Frontier Research in Chemistry (icFRC). The authors also thank the Spanish Ministry of Economy and Competitiveness, through projects FANCY CTQ2016-80030-R and the "Severo Ochoa" Programme for Centers of Excellence in R&D (SEV-2015-0496). This research was also supported by Generalitat de Catalunya (grant 2017SGR918).

Received: ((will be filled in by the editorial staff))
Revised: ((will be filled in by the editorial staff))
Published online: ((will be filled in by the editorial staff))

References

[1] X. Duan, C. Wang, A. Pan, R. Yu, X. Duan, *Chem. Soc. Rev.* **2015**, *44*, 8859.
[2] Y. Zhao, J. Qiao, Z. Yu, P. Yu, K. Xu, P. Lau Shu, W. Zhou, Z. Liu, X. Wang, W. Ji, Y. Chai, *Adv. Mater.* **2017**, *29*, 1604230.
[3] S. Z. Butler, S. M. Hollen, L. Cao, Y. Cui, J. A. Gupta, H. R. Gutierrez, T. F. Heinz, S. S. Hong, J. Huang, A. F. Ismach, E. Johnston-Halperin, M. Kuno, V. V. Plashnitsa, R. D. Robinson, R. S. Ruoff, S. Salahuddin, J. Shan, L. Shi, M. G. Spencer, M. Terrones, W. Windl, J. E. Goldberger, *ACS Nano* **2013**, *7*, 2898.
[4] S. B. Desai, S. R. Madhvapathy, A. B. Sachid, J. P. Llinas, Q. Wang, G. H. Ahn, G. Pitner, M. J. Kim, J. Bokor, C. Hu, H.-S. P. Wong, A. Javey, *Science* **2016**, *354*, 99.
[5] H. Liu, A. T. Neal, P. D. Ye, *ACS Nano* **2012**, *6*, 8563.
[6] Y. Liu, J. Guo, E. Zhu, L. Liao, S.-J. Lee, M. Ding, I. Shakir, V. Gambin, Y. Huang, X. Duan, *Nature* **2018**, *557*, 696.
[7] F. K. Perkins, A. L. Friedman, E. Cobas, P. M. Campbell, G. G. Jernigan, B. T. Jonker, *Nano Lett.* **2013**, *13*, 668.
[8] M. Sup Choi, G.-H. Lee, Y.-J. Yu, D.-Y. Lee, S. Hwan Lee, P. Kim, J. Hone, W. Jong Yoo, *Nat. Commun.* **2013**, *4*, 1624.
[9] S. Bertolazzi, D. Krasnozhon, A. Kis, *ACS Nano* **2013**, *7*, 3246.
[10] S.-Y. Cho, Y. Lee, H.-J. Koh, H. Jung, J.-S. Kim, H.-W. Yoo, J. Kim, H.-T. Jung, *Adv. Mater.* **2016**, *28*, 7020.
[11] M. Kim, N. S. Safron, C. Huang, M. S. Arnold, P. Gopalan, *Nano Lett.* **2012**, *12*, 182.
[12] M. Gobbi, S. Bonacchi, J. X. Lian, A. Vercouter, S. Bertolazzi, B. Zyska, M. Timpel, R. Tatti, Y. Olivier, S. Hecht, M. V. Nardi, D. Beljonne, E. Orgiu, P. Samorì, *Nat. Commun.* **2018**, *9*, 2661.
[13] H. Qiu, Y. Zhao, Z. Liu, M. Herder, S. Hecht, P. Samorì, *Adv. Mater.* **2019**, *31*, 1903402.
[14] Y. Zhao, S. Bertolazzi, P. Samorì, *ACS Nano* **2019**, *13*, 4814.
[15] Y. Zhao, S. Ippolito, P. Samorì, *Adv. Opt. Mater.* **2019**, *7*, 1900286.
[16] M. Min, S. Seo, S. M. Lee, H. Lee, *Adv. Mater.* **2013**, *25*, 7045.
[17] Z. Liu, A. A. Yasseri, J. S. Lindsey, D. F. Bocian, *Science* **2003**, *302*, 1543.
[18] M. Mas-Torrent, C. Rovira, J. Veciana, *Adv. Mater.* **2013**, *25*, 462.
[19] V. Parkula, M. S. Maglione, S. Casalini, Q. Zhang, P. Greco, C. A. Bortolotti, C. Rovira, M. Mas-Torrent, F. Biscarini, *Adv. Electron. Mater.* **2019**, *5*, 1800875.
[20] Z. Yu, Y. Pan, Y. Shen, Z. Wang, Z.-Y. Ong, T. Xu, R. Xin, L. Pan, B. Wang, L. Sun, J. Wang, G. Zhang, Y. W. Zhang, Y. Shi, X. Wang, *Nat. Commun.* **2014**, *5*, 5290.
[21] S. Bertolazzi, S. Bonacchi, G. Nan, A. Pershin, D. Beljonne, P. Samorì, *Adv. Mater.* **2017**, *29*, 1606760.
[22] S. Mignuzzi, A. J. Pollard, N. Bonini, B. Brennan, I. S. Gilmore, M. A. Pimenta, D. Richards, D. Roy, *Phys. Rev. B* **2015**, *91*, 195411.
[23] S. Tongay, J. Suh, C. Ataca, W. Fan, A. Luce, J. S. Kang, J. Liu, C. Ko, R. Raghunathanan, J. Zhou, F. Ogletree, J. Li, J. C. Grossman, J. Wu, *Sci. Rep.* **2013**, *3*, 2657.
[24] M. M. Perera, M.-W. Lin, H.-J. Chuang, B. P. Chamlagain, C. Wang, X. Tan, M. M.-C. Cheng, D. Tománek, Z. Zhou, *ACS Nano* **2013**, *7*, 4449.
[25] A. Allain, A. Kis, *ACS Nano* **2014**, *8*, 7180.
[26] I. Ferain, C. A. Colinge, J.-P. Colinge, *Nature* **2011**, *479*, 310.
[27] S. M. Sze, K. K. Ng, in *Physics of Semiconductor Devices*, John Wiley & Sons, Inc., **2006**, 293.
[28] X. Chia, A. Ambrosi, D. Sedmidubský, Z. Sofer, M. Pumera, *Chem. Eur. J.* **2014**, *20*, 17426.
[29] Y. Wang, C.-H. Kim, Y. Yoo, J. E. Johns, C. D. Frisbie, *Nano Lett.* **2017**, *17*, 7586.

[30] E. Marchante, N. Crivillers, M. Buhl, J. Veciana, M. Mas-Torrent, *Angew. Chem., Int. Ed.* **2016**, *55*, 368.
[31] C. L. Bentley, J. Li, A. M. Bond, J. Zhang, *J. Phys. Chem. C* **2016**, *120*, 16516.
[32] K. F. Mak, K. He, C. Lee, G. H. Lee, J. Hone, T. F. Heinz, J. Shan, *Nat. Mater.* **2012**, *12*, 207.
[33] S. Mouri, Y. Miyauchi, K. Matsuda, *Nano Lett.* **2013**, *13*, 5944.
[34] A. M. Ionescu, H. Riel, *Nature* **2011**, *479*, 329.
[35] D. Sarkar, X. Xie, W. Liu, W. Cao, J. Kang, Y. Gong, S. Kraemer, P. M. Ajayan, K. Banerjee, *Nature* **2015**, *526*, 91.
[36] K. Gopalakrishnan, P. B. Griffin, J. D. Plummer, *IEEE Trans. Electron Devices* **2005**, *52*, 69.
[37] N. Abele, R. Fritschi, K. Boucart, F. Casset, P. Ancey, A. M. Ionescu, presented at 2005 IEEE Int. Electron Devices Meeting (IEDM), Washington, DC, December **2005**.
[38] F. A. McGuire, Y.-C. Lin, K. Price, G. B. Rayner, S. Khandelwal, S. Salahuddin, A. D. Franklin, *Nano Lett.* **2017**, *17*, 4801.
[39] X. Liu, R. Liang, G. Gao, C. Pan, C. Jiang, Q. Xu, J. Luo, X. Zou, Z. Yang, L. Liao, Z. L. Wang, *Adv. Mater.* **2018**, *30*, 1800932.
[40] A. I. Khan, K. Chatterjee, B. Wang, S. Drapcho, L. You, C. Serrao, S. R. Bakaul, R. Ramesh, S. Salahuddin, *Nat. Mater.* **2014**, *14*, 182.
[41] M. Hoffmann, F. P. G. Fengler, M. Herzig, T. Mittmann, B. Max, U. Schroeder, R. Negrea, P. Lucian, S. Slesazeck, T. Mikolajick, *Nature* **2019**, *565*, 464.
[42] A. Daus, C. Vogt, N. Münzenrieder, L. Petti, S. Knobelspies, G. Cantarella, M. Luisier, G. A. Salvatore, G. Tröster, *IEEE Trans. Electron Devices* **2017**, *64*, 2789.
[43] X. P. A. Gao, G. Zheng, C. M. Lieber, *Nano Lett.* **2010**, *10*, 547.

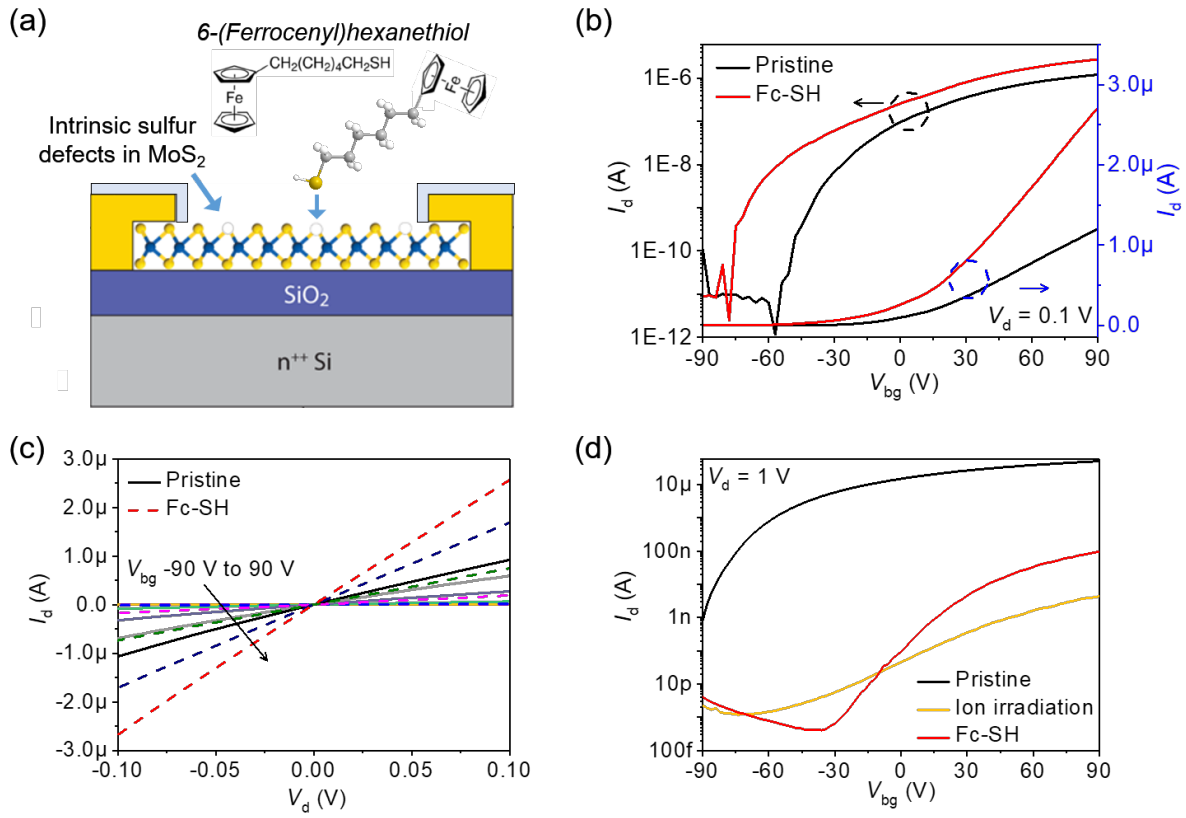

Figure 1. (a) Schematic diagram of back-gate monolayer MoS_2 FET with adsorbed 6-(ferrocenyl)hexanethiol (Fc-SH) molecules. (b) Transfer characteristics of back-gate monolayer MoS_2 FET before and after exposure to Fc-SH molecules. (c) Output characteristics of back-gate monolayer MoS_2 FET before and after exposure to Fc-SH molecules. (d) Transfer characteristics of back-gate monolayer MoS_2 FET in the pristine state, with generated defects by ion irradiation, and finally after molecular healing.

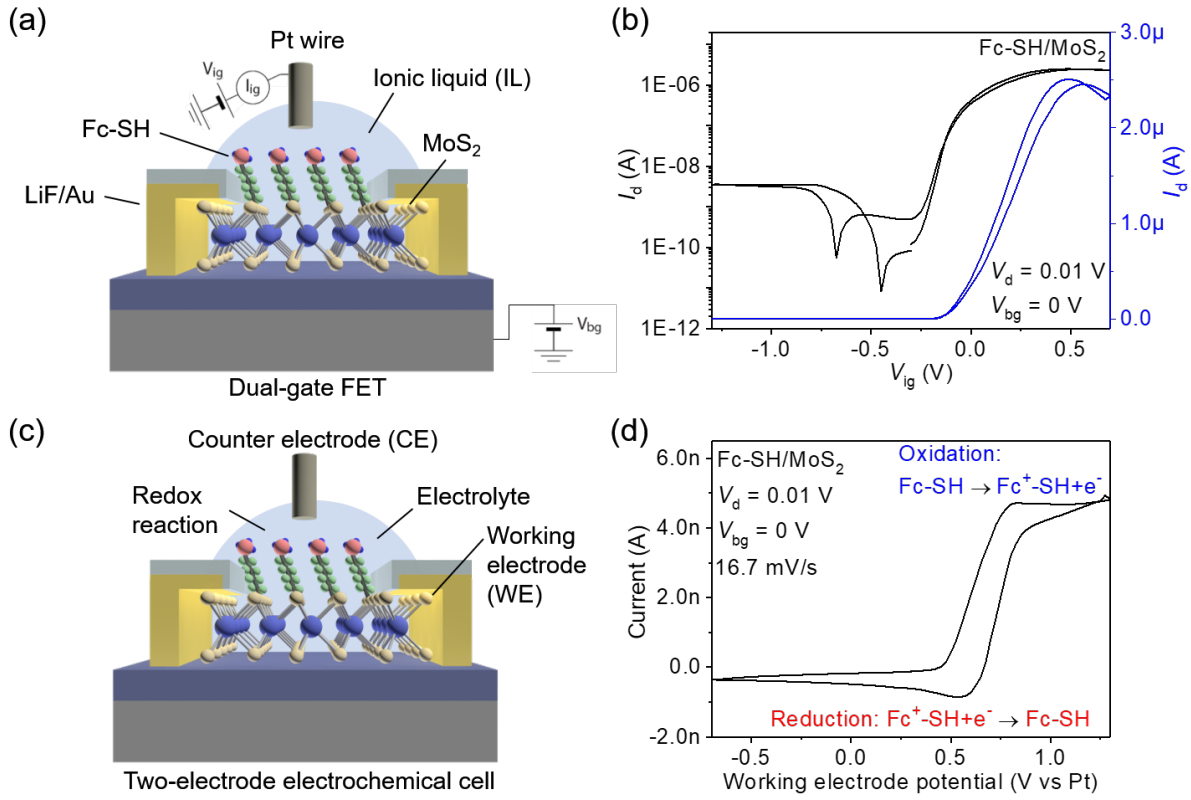

Figure 2. (a) Schematic diagram of IL-gated monolayer MoS_2 FET with adsorbed Fc-SH molecules. (b) Transfer characteristics of IL-gated monolayer MoS_2 FET with adsorbed Fc-SH molecules. Channel length/width is 4.2 μm/3.4 μm. (c) Schematic diagram of two-electrode electrochemical cell with monolayer MoS_2 FET as working electrode. (d) The cyclic voltammogram of Fc-SH at the MoS_2/IL interface.

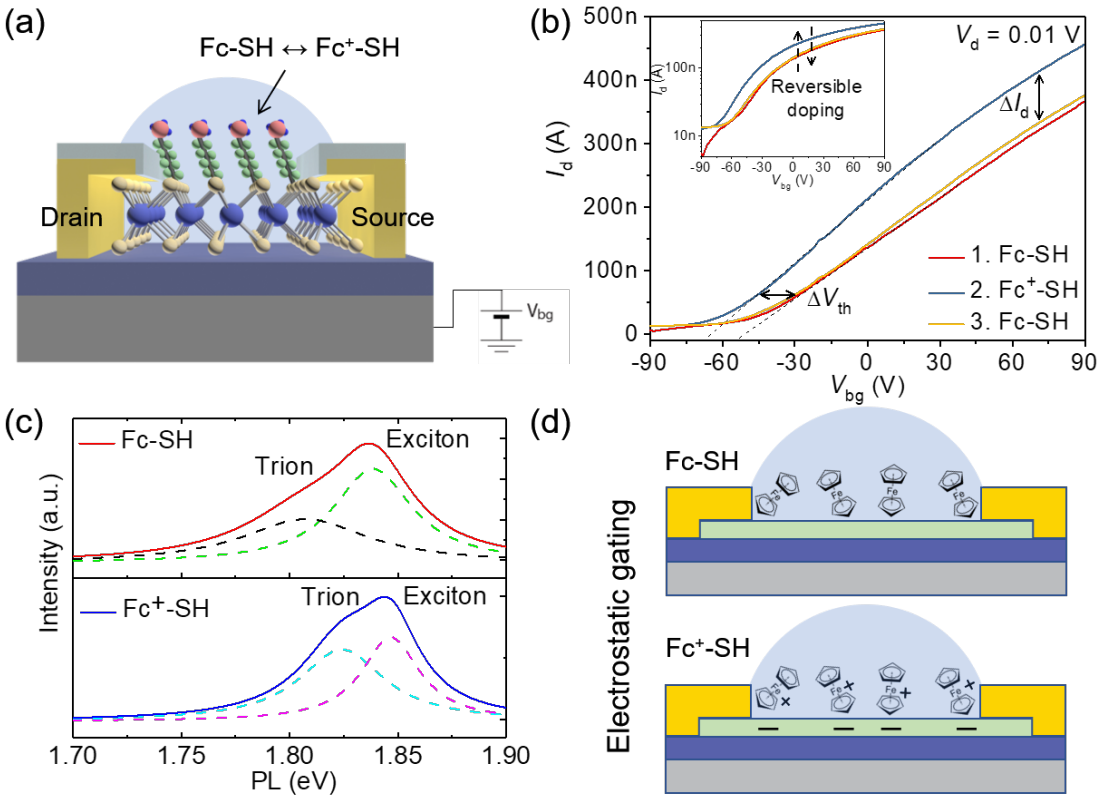

Figure 3. (a) Schematic diagram of monolayer MoS_2 FET with adsorbed Fc-SH molecules at neutral or charged state. (b) Back-gate transfer characteristics of monolayer MoS_2 FET with different Fc-SH electrochemical states in the linear scale. Inset shows the transfer curves in the logarithmic scale. (c) The comparison of PL spectra of monolayer MoS_2 with the adsorption of Fc-SH or Fc^+-SH molecules. The A peak is fitted with neutral excitons and negatively charged trions. (d) A schematic diagram shows the controllable and reversible doping of MoS_2 by switching the molecular electrochemical state.

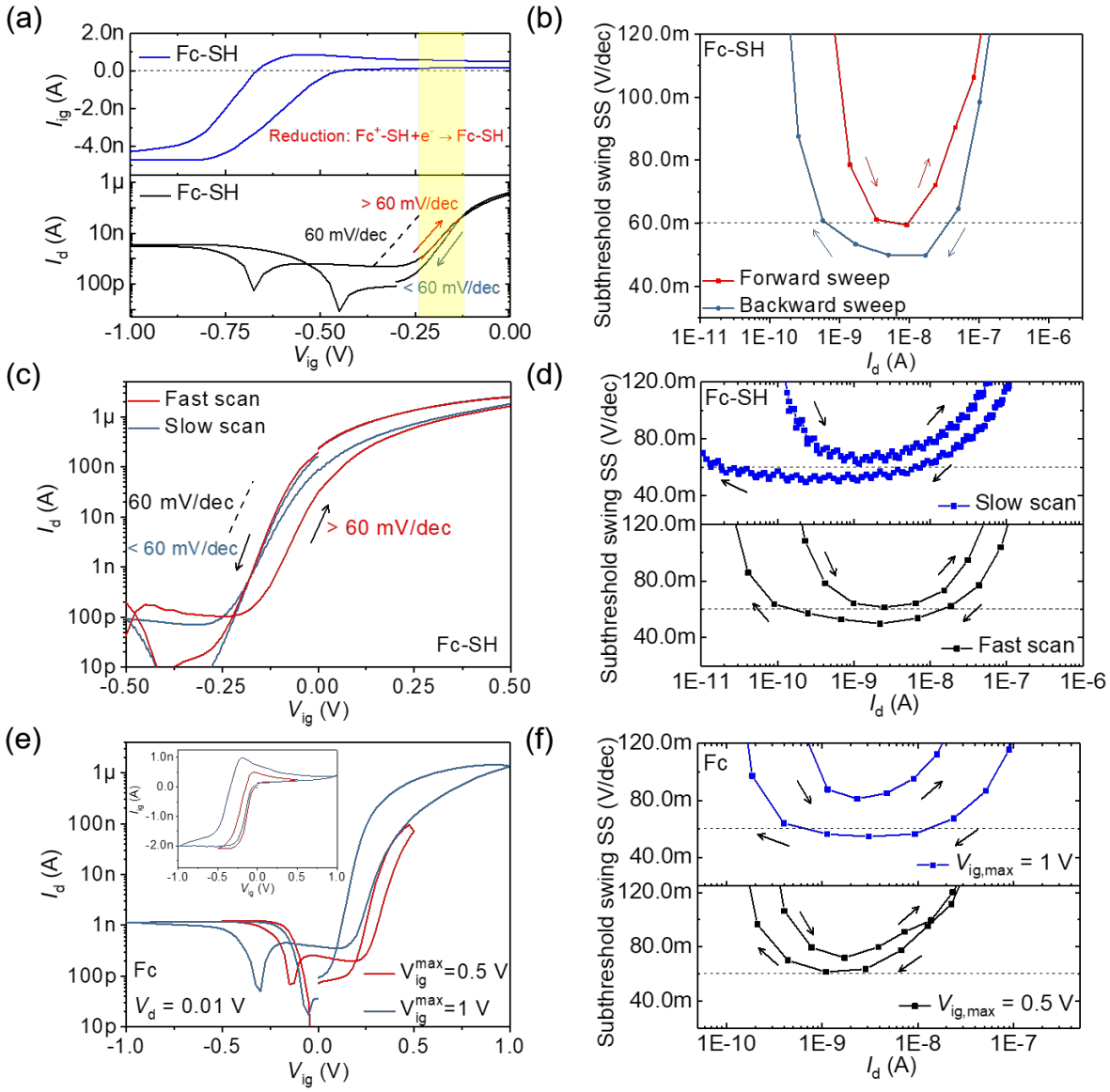

Figure 4. (a) Plot of transfer curve and IL-gate current under the same IL-gate voltage in the MoS_2 FET with Fc-SH adsorption, demonstrating the function of molecules in the reduced SS effect. (b) Plot of SS with drain current of MoS_2 FET with adsorbed Fc-SH molecules in the forward and backward sweep of IL-gated voltage. (c) Plot of transfer curve under different scan rate of IL-gate voltage. (d) Plot of SS with drain current under different scan rate of IL-gate voltage. (e) Plot of transfer curve and IL-gate current (inset) under different scan range of IL-gate voltage. (f) Plot of SS with drain current under different scan range of IL-gate voltage.